Magnetic properties of high-T_c superconducting grains

Du-Xing Chen and Alvaro Sanchez
Electromagnetism Group, Physics Department, Universitat Autònoma de Barcelona, 08193 Bellaterra, Spain
(Received 6 December 1991)

A phenomenological model has been developed for interpreting the magnetic properties of hard type-II superconductors. By means of a volume and a surface supercurrent density, this model considers the effects of the bulk flux pinning, the thermal equilibrium magnetization, and the surface barrier. Based on this model, several difficult problems concerning the explanation of the hysteresis loop and susceptibility data of high-T_c superconducting grains are solved. Our work demonstrates the presence of a surface-barrier effect in high-T_c superconductors. Accordingly, some past work on H_{c1} and J_c determination and ac loss mechanisms should be reinterpreted.

Recently, Lam *et al.*[1] reported results of complex permeability $\mu = \mu' - j\mu''$ as a function of ac field amplitude H_m for a sintered $YBa_2Cu_3O_7$ (Y 1:2:3) sample in a wide field range covering two μ'' peaks. The first (low-field) peak is due to the intergranular supercurrents and the second one to the supercurrents inside the grains. They used a field-dependent critical-state model to simulate the second peak, and found that the predicted μ'' had to be reduced by a factor of 3 to better compare the shape of the data. Even so, the theoretical μ'' peak was sharper, and the corresponding μ' curve was shifted to the low-field side of the data by 30%. They remarked that this was a problem too complex to treat. Similar problems have been found and discussed in terms of complex susceptibility and induced emf wave form by other authors without a proper solution.[2-4] On the other hand, it is well known that at temperatures not too low the high-field hysteresis loops of sintered high-T_c superconductors have a tilted Z shape.[5] The explanation of such a loop shape has also been thought to be a difficult task. In this paper we will argue that all the above phenomena originate from the presence of thermal equilibrium magnetization and a surface barrier in the high-T_c superconducting grains. We also present a model by which the difficulties mentioned above can be solved.

Figure 1(a) shows some hysteresis loops of a Y 1:2:3 sample (S1) measured with a vibrating sample magnetometer at 76 K.[6] We see that the high-H_m loops have a tilted Z shape with maximum width ΔM at the two bending positions. This loop shape cannot be predicted by the critical-state model with any realistic internal-field-dependent critical-current density $J_c(H_i)$.[7-9]

In the critical-state loops, the magnetization M is due to the penetrated volume supercurrents induced by the applied field H. If H_m is large enough, the middle section for either the ascending or the descending branch corresponds to the full penetration state in which the supercurrents circulate in the same direction. Thus, for a given H the M values on the two branches should be close to each other with opposite signs, resulting in a loop almost symmetric with respect to the H axis. This means that for the critical-state loop, the middle line between the two branches roughly collapses with the H axis, and the Z-shaped experimental loop cannot be explained by the volume supercurrents. This middle line can be regarded as the reversible component of the loop. Obviously, the reversible Z-shaped middle line is due to the thermal equilibrium magnetization curve $M_{eq}(H)$ of the type-II superconductor, which has a 180-degree rotation symmetry containing a linear interval between $-H_{c1}$ and H_{c1}.[6]

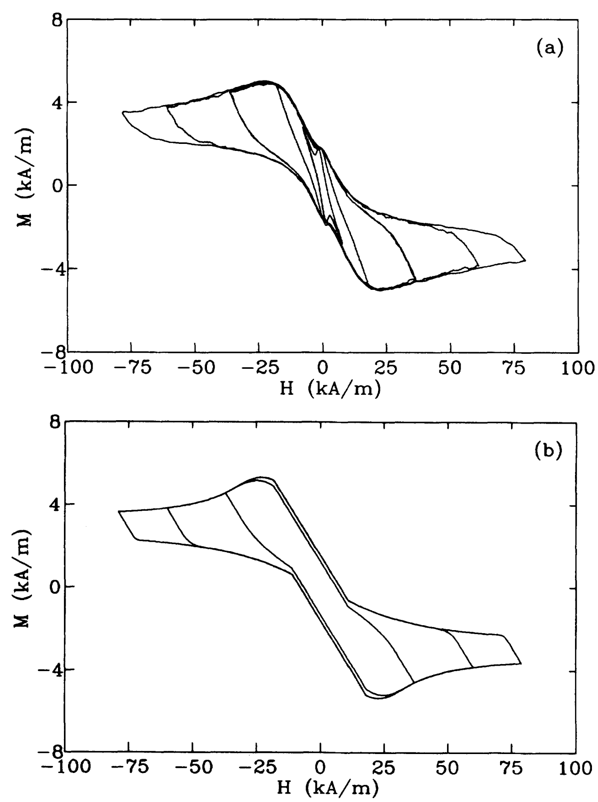

FIG. 1. (a) High-field dc hysteresis loops at 76 K for a Y 1:2:3 sample (S1); (b) their model fit for higher H_m.

Since the local J_c decreases with increasing $|H_i|$, the spatially averaged J_c decreases with increasing $|H|$, and so does ΔM for the critical-state loop. The two observed ΔM maxima around $\pm H_{c1}$ suggest that there is an additional loss mechanism which has a large function around $\pm H_{c1}$. It is well known from conventional type-II superconductor research that the ac loss mechanism for volume supercurrents is vortex depinning from the defects, which is expressed phenomenologically by the critical-state model.[10,11] The vortices can also be pinned on the sample surface, and this surface pinning makes the flux enter the sample at $H > H_{c1}$ and exit at $H < H_{c1}$. Thus, some ac losses arise even without defects serving as internal pinning centers. In other words, there is a potential barrier at the surface (surface barrier) which requires extra field increments $\Delta H_{\rm en}$ and $\Delta H_{\rm ex}$ for the flux entering and exiting the sample.[12,13]

Clem[13] discussed the above two extra factors theoretically, and together with the volume supercurrents he made a critical-state theory for type-II superconductors. He described J_c, $\Delta H_{\rm en}$, and $\Delta H_{\rm ex}$ as decreasing functions of B, the local averaged flux density. However, no hysteresis loops were calculated using this theory, so no comparison was made between theoretical loops and experimental data. LeBlanc[14] calculated some simple loops assuming both J_c and $\Delta H(=\Delta H_{\rm en}=\Delta H_{\rm ex})$ to be constant. His results illustrate some concepts, but it is almost impossible to use them for comparison with experimental data.

Hence, in order to understand the relation between the experimental loops and their three origins, we have to make a model including several parameters sufficient to display the effects of these origins. Following Fietz *et al.*,[15] who have treated the critical-state model together with the equilibrium magnetization, and Dunn *et al.*,[16] whose calculation considered all three factors with a constant ΔH and a constant $M_{\rm eq}$ above H_{c1}, the main points of our treatment[6] are described as follows.

An infinitely long cylinder of a hard type-II superconductor is modeled as a core surrounded by a tube of thickness λ, the London penetration depth. The penetrated volume supercurrents, with a density equal to the critical-current density J_c (A/m^2), flow in the core, while the surface current with a density j_s (A/m, for unit longitudinal length) flows in an infinitely thin sheath, which is in the tube and adjacent to its inner boundary. When H is cycling between H_m and $-H_m$, the j_s versus H curve forms a hysteresis loop, reflecting the thermal equilibrium magnetization and the surface barrier effect. From the definition of j_s, we have

$$j_s = M_s, \tag{1}$$

$$H_e = H + j_s, \tag{2}$$

where M_s is the magnetization in the core contributed by j_s and H_e is the boundary field of the core. The $j_s(H)$ loop has a 180-degree rotation symmetry. For $H \geq 0$, the ascending j_s versus H curve has a linear section with a slope of -1 from the zero point to a field H_1 larger than H_{c1}, while the descending curve from a high H_m collapses with this section after H is less than a field H_2 which is smaller than H_{c1}. That $H_1 > H_2$ is due to the presence of the surface barrier. For simplicity we assume that the extra field increments for flux entry and exit are equal, so that

$$\Delta H_0 = (H_1 - H_2)/2, \tag{3}$$

$$H_{c1} = (H_1 + H_2)/2, \tag{4}$$

where ΔH_0 is ΔH at $B \approx 0$. The other sections of the $j_s(H)$ loop are assumed to be of exponential type.[6]

The magnetization $M(H)$ for the core is calculated as the sum of the volume current and the surface current contributions, M_c and M_s:

$$M(H) = M_c(H_e(H)) + M_s(H). \tag{5}$$

In the calculation of M_c, an exponential $J_c(H_i)$ function is used:[8]

$$J_c(H_i) = J_c(0)\exp(-|H_i|/H_0); \tag{6}$$

the boundary field is taken to be H_e. An important parameter here is the full penetration field H_p, characterizing the total circulating volume supercurrent when the core is just fully penetrated from the initial state.

The total $M(H)$ for the cylinder is less than the one calculated from Eq. (5) by a factor equal to the volume ratio of the core to the whole cylinder. The same thing has to be done when applying the model to the grains in a sintered sample; the effective grain volume fraction g, less than 1, is the factor in this case.[4]

Performing the above treatment we fit the loops given in Fig. 1(a). The results are shown in Fig. 1(b). Some fitting parameters are listed in Table I. The average grain radius $a_g = 3.5\ \mu$m.[6]

A good agreement can be seen from the experimental and the model-fitting loops. This confirms the presence of a surface barrier effect for the high-T_c superconducting grains and shows the importance of the consideration of all three determining factors. Similar results have been obtained for several other samples, some of which have much smaller H_p, so that the surface barrier has a dominant effect on the ac losses.

We next treat the high-field χ'' based on the same idea. For practical reasons, we use a slightly simplified model,

TABLE I. The fitting parameters for S1 and S2.

Sample	H_{c1} (kA/m)	ΔH_0 (kA/m)	H_p (kA/m)	M_r (kA/m)	g	f
S1	14.5	3.5	19	1.3[a]	0.20	
S2	9.46	2.68		1.566	0.66	0.153

[a] Calculated from the fitting parameters.

where the loop is approximated by closed linear sections as shown in Fig. 2(a).[17] As a result, the following equation can be used satisfactorily for a field region around the χ'' peak:

$$\chi''(H_m) = AH_m^{-2} + BH_m^{-1} + C, \tag{7}$$

where A, B, and C are constants. They are related to H_1, H_2, M_r (the remanence of the loop), g (= $\tan\alpha$), and another quantity f (= $\tan\beta$), characterizing the field dependence of ΔH and J_c, by

$$A = \{ (f+g)(H^{*2} - H_1^2) + (1 + f/g)fH^{*2} \\ -2(1+f/g)[(f+g)H_1 - gH_2 + 2M_r]H^*\}/\pi, \tag{8}$$

$$B = 2(1+f/g)[(f+g)H_1 - gH_2 + 2M_r]/\pi, \tag{9}$$

$$C = -(1+f/g)f/\pi, \tag{10}$$

where

$$H^* = H_1 + 2M_r/(f+g). \tag{11}$$

In Fig. 2(b) we redraw the data for the sintered Y 1:2:3 in Ref. 1 in terms of susceptibility.[17] The fit using Eq. (7) for the second χ'' peak is also given, showing a good agreement. From the fitting parameters A, B, and C, together with the value of χ' corresponding to the $\chi''_{\rm max}$, a set of final model parameters are unambigously obtained using Eqs. (8)–(11); they are listed in Table I. The loop shown in Fig. 2(a) corresponds to these parameters. We note here that the H_m for the second $\chi''_{\rm max}$ is 19 kA/m, and the average grain radius a_g = 10 μm, according to Ref. 1.

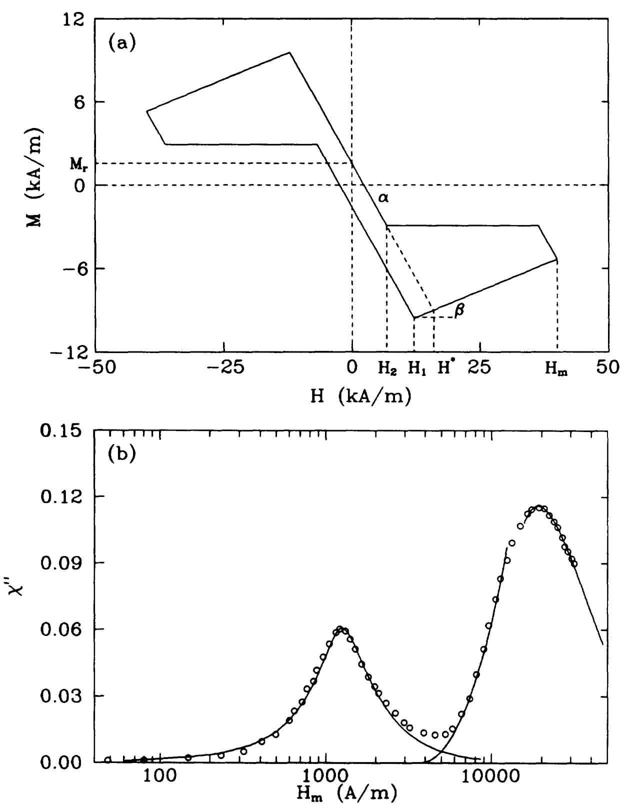

FIG. 2. (a) A simplified high-H_m model loop; (b) the measured $\chi''(H_m)$ curve at 77 K for a Y 1:2:3 sample (S2) and the model result. The second peak is fitted by using Eq. (7). (The first intergranular peak is fitted by the exponential critical-state model. The rising side of the second peak is modeled by a modified Rayleigh-law dependence.)

Thus, the main part of the $\chi''(H_m)$ and $\chi'(H_m)$ curves has been successfully interpreted by the model loops. The main consequences of this model are $H_m(\chi''_{\rm max})$ is determined not only by J_c but also by H_{c1} and ΔH_0; it increases with increasing H_{c1} and ΔH_0. For $\chi''_{\rm max}$ there is another influencing factor g; the value of $\chi''_{\rm max}$ increases with increasing ΔH_0, J_c, and g.

We now check the validity of our model by comparing two ways to calculate the average intragranular critical-current density $\langle J_{cg}\rangle$. The formulas are[4,7]

$$\langle J_{cg}\rangle = H_p/a_g, \tag{12}$$

$$\langle J_{cg}\rangle = 3M_r/a_g g. \tag{13}$$

Using the fitting parameters of S1 given in Table I and its a_g, we obtain $\langle J_{cg}\rangle$ = 5400 MA/m^2 from Eq. (12) and 5600 MA/m^2 from Eq. (13). The two values are similar, showing the self-consistency of the model. In practice, we can use Eq. (13) to determine $\langle J_{cg}\rangle$, since all the values in this formula are easy to obtain even without a detailed model fit.

From susceptibility measurements, the conventional way to determine $\langle J_{cg}\rangle$ is based on

$$\langle J_{cg}\rangle = H_m(\chi''_{\rm max})/a_g. \tag{14}$$

This gives $\langle J_{cg}\rangle$ = 1900 MA/m^2 for S2. With the results of our model fit, the value of $\langle J_{cg}\rangle$ calculated using Eq. (13) is 710 MA/m^2. The correct value should be the latter, for the following reason. The $\chi''(H_m)$ curve cannot be fitted by the critical-state model which is the basis of Eq. (14), while our model fits well the data so Eq. (13) is valid. Actually, if we let M_r = 0 and keep the other fitting parameters the same, the $\langle J_{cg}\rangle$ will be 2000 MA/m^2 from the resultant $H_m(\chi''_{\rm max})$ using Eq. (14). In other words, $H_m(\chi''_{\rm max})$ and $\langle J_{cg}\rangle$ calculated from Eq. (14) *increase with decreasing* J_{cg}, and this has obviously no physical meaning.

By comparing the hysteresis loop and the modeling loop, our work has detected the presence of a surface barrier in high-T_c superconducting grains. From the loop fit of a grain aligned Y 1:2:3 sample, we found ΔH to be anisotropic; it is only present when the field is along the c axis. Moreover, there are some published data which imply that it is not always present in all the high-T_c superconductors. Therefore, further study is needed on the mechanism of such a surface barrier; it may be different from that in conventional superconductors.[18]

In conclusion, we have presented a model and used it to interpret the high-field hysteresis loops and ac susceptibility data of high-T_c superconductors. This model considers the effects of volume supercurrents, the thermal equilibrium magnetization, and the surface barrier for flux entry and exit. We see that all the difficult problems mentioned earlier have been solved by appeal to our model. An important quantity for the high-T_c grains is the intragranular $\langle J_c \rangle$. Its correct determination should be made based on such a model. Since the effect of the surface barrier was not considered in high-T_c superconductors, all previous determinations of H_{c1} for high-T_c grains or crystals[19] have actually been for $H_1 = H_{c1} + \Delta H_0$. A separation of the contributions from J_c, H_{c1}, and ΔH is needed for the study of magnetic properties of high-T_c superconducting grains. The present model and related concepts provide a tool to do this. Moreover, the model allows the study of the properties of the grains simultaneously with intergrain coupling, for a large number of sintered samples made from different techniques. This is important since the intrinsic properties of the grains, which influence directly the coupling, are sensitive to the sample preparation conditions; they are different from those of single crystals, which are grown and annealed under special conditions. Nevertheless, our treatment is also valid in principle for single crystals, although complicated demagnetizing effects have to be considered in this case.

We thank R. B. Goldfarb and J. S. Muñoz for their support, and R. W. Cross for help in dc magnetic measurements. We are grateful to J. R. Clem and M. Suenaga for their comments. One of us (D.X.C.) thanks the Ministerio Español de Educación y Ciencia for financial support for his stay. Support from Spanish Superconductivity Program MIDAS and CIRIT is also acknowledged.

[1] Q.-H. Lam, Y. Kim, and C. D. Jeffries, Phys. Rev. B **42**, 4846 (1990).

[2] H. Kupfer *et al.*, Cryogenics **28**, 650 (1988).

[3] K.-H. Muller, Physica C **159**, 717 (1989).

[4] D.-X. Chen, A. Sanchez, T. Puig, L. M. Martinez, and J. S. Muñoz, Physica C **168**, 652 (1990).

[5] A. Ding, Z. Yu, K. Shi, and J. Yan, Physica C **153-155**, 1509 (1988); H. Dersch and G. Blatter, Phys. Rev. B **38**, 11 391 (1988); P. Chaddah *et al.*, Cryogenics **29**, 907 (1989).

[6] D.-X. Chen, R. W. Cross, and A. Sanchez (unpublished).

[7] D.-X. Chen and R. B. Goldfarb, J. Appl. Phys. **66**, 2510 (1989).

[8] D.-X. Chen, A. Sanchez, and J. S. Muñoz, J. Appl. Phys. **67**, 3430 (1989).

[9] D.-X. Chen, A. Sanchez, J. Nogues, and J. S. Muñoz, Phys. Rev. B **41**, 9510 (1990).

[10] C. P. Bean, Phys. Rev. Lett. **8**, 250 (1962).

[11] Y. B. Kim, C. F. Hempstead, and A. R. Strnad, Phys. Rev. Lett. **9**, 306 (1962).

[12] C. P. Bean and J. D. Livingston, Phys. Rev. Lett. **12**, 14 (1964).

[13] J. R. Clem, J. Appl. Phys. **50**, 3518 (1979).

[14] M. A. R. LeBlanc and J. P. Lorrain, Cryogenics **24**, 143 (1984).

[15] W. A. Fietz, M. R. Beasley, J. Silcox, and W. W. Webb, Phys. Rev. **136**, A335 (1964).

[16] W. I. Dunn and P. Hlawiczka, Br. J. Appl. Phys. **1**, 1649 (1968).

[17] D.-X. Chen and A. Sanchez, in *Susceptibility of Superconductors and Other Spin Systems*, edited by T. L. Francavilla *et al.* (Plenum, to be published).

[18] A. M. Campbell and J. E. Evetts, Adv. Phys. **21**, 199 (1972).

[19] For example, L. Krusin-Elbaum, A. P. Malozemoff, Y. Yeshurun, D. C. Cronemeyer, and F. B. Holtzberg, Phys. Rev. B **39**, 2936 (1989); Dong-Ho Wu and S. Sridhar, Phys. Rev. Lett. **65**, 2074 (1990).